L1/L5 SBAS MOPS Ephemeris Message to Support Multiple Orbit Classes

Tyler Reid*, Todd Walter, & Per Enge
Stanford University
*Email: tyreid@stanford.edu

BIOGRAPHY

Tyler Reid is a Ph.D. candidate in the GPS Research Laboratory working under the guidance of Professor Per Enge and Dr. Todd Walter in the Department of Aeronautics and Astronautics at Stanford University. He received his B.Eng. in Mechanical Engineering from McGill University, Montreal, Canada in 2010 and his M.Sc. in Aeronautics and Astronautics from Stanford University in 2012. He is also an alumnus of the International Space University (ISU) Space Studies Program (SSP) of 2011 held at the Technical University of Graz in Austria. His research interests are in global navigation satellite and augmentation systems, orbital mechanics, and space applications.

Todd Walter is a senior research engineer in the GPS Research Laboratory in the Department of Aeronautics and Astronautics at Stanford University. He received his Ph.D. from Stanford in 1993 and has worked extensively on the Wide Area Augmentation System (WAAS). He is currently working on dual-frequency, multi-constellation solutions for aircraft guidance. He received the Thurlow and Kepler awards from the ION. He is also a fellow of the ION and currently serves as its president.

Per Enge is a Professor of Aeronautics and Astronautics at Stanford University, where he is the Vance and Arlene Coffman Professor in the School of Engineering. Here, he directs the GPS Research Laboratory which develops navigation systems based on the Global Positioning System (GPS). He has been involved in the development of WAAS and LAAS for the Federal Aviation Administration (FAA). He has received the Kepler, Thurlow, and Burka Awards from the ION. He also received the Summerfield Award from the American Institute of Aeronautics and Astronautics (AIAA) as well as the Michael Richey Medal from the Royal Institute of Navigation. He is a fellow of the Institute of Electrical and Electronics Engineers (IEEE), a fellow of the ION, a member of the National Academy of Engineering, and has been inducted into the Air Force GPS Hall of Fame. He received his Ph.D. from the University of Illinois in 1983.

ABSTRACT

New satellite orbits ranging from highly eccentric inclined geosynchronous (IGSO), medium (MEO) to low Earth (LEO) orbits are being proposed for future Global Navigation Satellite Systems (GNSS) and Satellite Based Augmentation Systems (SBAS). This paper addresses the challenges associated with designing a message for the L5 Minimum Operational Performance Standards (MOPS) ephemeris and almanac data which can handle this broad spectrum of proposed orbital regimes. In the past, the MOPS message used Earth fixed Cartesian position, velocity, and acceleration (9 degrees-of-freedom (DOF)) to describe the motion of the geostationary (GEO) SBAS satellites. The proposed next generation MOPS message will have to be much more sophisticated in order to encompass potential navigation and augmentation satellites ranging from GSO to LEO. A method of optimally fitting orbital elements has been devised which allows for a wide variety of orbital elements to be employed. With this, a 9 DOF set of orbital elements has been selected for the ephemeris message and a 7 DOF set for the almanac which function amicably for the range of orbits in question. Case studies show the effectiveness of the proposed message for GPS, GLONASS, BeiDou, WAAS, EGNOS, QZSS, Iridium, and other proposed orbits such as Molniya. Quantization and detailed message structure will also be discussed.

INTRODUCTION

GPS has launched its first two L5 capable satellites and is slated to achieve its L5 Full Operational Capability (FOC) by the year 2019. GLONASS has returned to a full constellation of 24 operational satellites and has plans to offer CDMA signals at both the L1 and L5 frequencies. The European Galileo and Chinese Beidou constellations are currently under construction and also intend to broadcast in both the L1 and L5 bands. Thus, it is possible that in the next decade, there could be four constellations suitable for use in aviation with signals at L1 and L5. RTCA is developing an update to the Satellite Based Augmentation System (SBAS) Minimum Operational Performance Standards (MOPS) to include the use of GPS

L5. EUROCAE is similarly developing dual frequency MOPS for Galileo. The intent is that these two efforts will be merged into a single MOPS [1].

The different SBAS service providers have formed an Interoperability Working Group (IWG) to ensure that their respective systems remain compatible as well as to plan for future enhancements. This group has set a goal of having the next MOPS support all four constellations [1].

It is desired that the L5 MOPS message not be limited to distribution by geostationary (GEO) satellites, a limitation set by the current ephemeris (Message Type 9) and almanac (Message Type 17) messages. There are a large number of new orbits now being utilized by GNSS and SBAS systems as well as others on the horizon and developing a message capable of supporting all of them is the goal of this paper.

Navigation and augmentation satellites have been placed in trajectories ranging from low Earth orbits (LEO) all the way out to geosynchronous (GSO). Figure 1 shows past, present, and future navigation satellites and augmentation systems at their nominal operational altitudes. Early satellite navigation systems such as the US Transit (operational from 1964-1996) and Soviet Cicada (operational from 1976-present) were placed in LEO. As such, it is not unimaginable that navigation or augmentation services be offered from LEO in the future. In fact, there has been considerable interest in using the Iridium satellite phone constellation for this very application, for example [2].

Medium Earth orbits have now been employed by all GNSS systems including the fully operational GPS and GLONASS constellations as well as those of Galileo and BeiDou which are currently in the construction phase. Additional geometry has been added by the BeiDou system via the inclusion of GEO and inclined GSOs (IGSO). Making use of the 24 period of these orbits, these satellites are always over China, giving rise to a regional service with only 10 satellites in 2011.

Augmentation systems such as the US WAAS, European EGNOS, and Japanese MSAS, i.e. those which broadcast the MOPS message currently civil aviation purposes, are placed in GEO. However, new augmentation systems such as Japan's Quasi-Zenith Satellite System offer GPS augmentation to improve geometry for users in cities with tall skyscrapers where the urban canyon effect limits GPS-only performance. QZSS is not only an IGSO, it also has a considerable eccentricity which gives rise to the satellite spending most of its time over the northern hemisphere and Japan. Other types of orbits are also being considered for augmentation. Originally used for high latitude communications, highly eccentric orbits (HEO) such as Molniya orbits are being considered for Arctic integrity where current SBAS GEOs are below the horizon and cannot be seen [3].

Figure 2 shows all of the trajectories used by GNSS and SBAS today as well as the Iridium constellation to give a sense of the relative scales of LEO, MEO, and GSO. This variety of complex trajectories requires a more general message than the Cartesian Earth fixes position, velocity, and acceleration provided by the current MOPS. This paper demonstrates that it is feasible to design a message based on orbital elements which can support the various orbits being used in GNSS and augmentation today as well as many of those being considered for the future.

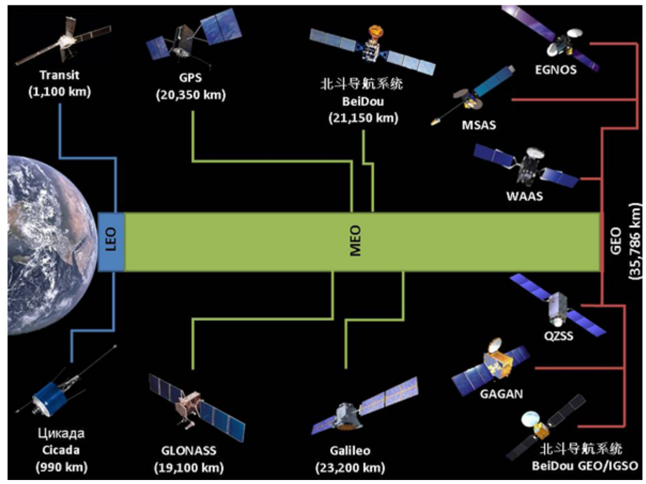

Figure 1: GNSS orbit classes

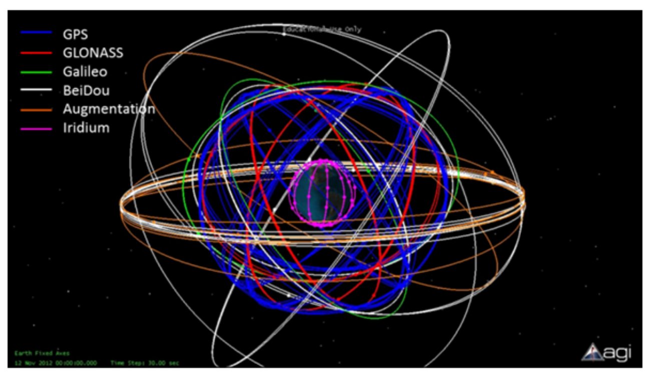

Figure 2: All GNSS satellites and augmentation systems plus Iridium

CURRENT MOPS MESSAGE & LIMITATIONS

Ephemeris

The current SBAS MOPS GEO ephemeris message (MT 9) describes the position of Geostationary (GEO) satellites accurately over a short period of time so that these satellites can be used for ranging and included in the position solution. The message makes use of 9 parameters, Earth Centered Earth Fixed (ECEF) Cartesian position, velocity, and acceleration, to describe the motion of the GEO satellites from which the MOPS message is broadcast. This message is updated every 2 minutes and is valid for a maximum of 6 minutes. This ephemeris message has the structure shown in Figure 3 below.

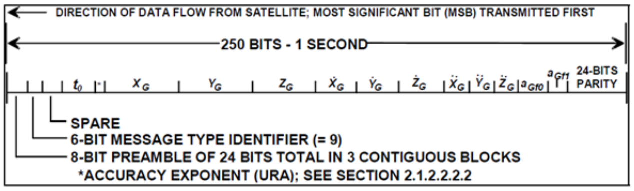

Figure 3: Type 9 GEO ephemeris message format [4]

Parameter	No. of Bits (Note 1)	Scale Factor (LSB)	Effective Range (Note 1)	Units
Reserved	8			
t_0	13	16	0 to 86,384	seconds
URA (Note 2)	4	(Note 2)	(Note 2)	(Note 2)
X_G (ECEF)	30	0.08	±42,949,673	meters
Y_G (ECEF)	30	0.08	±42,949,673	meters
Z_G (ECEF)	25	0.4	±6,710,886.4	meters
X_G Rate-of-Change	17	0.000625	±40.96	meters/sec
Y_G Rate-of-Change	17	0.000625	±40.96	meters/sec
Z_G Rate-of-Change	18	0.004	±524.288	meters/sec
X_G Acceleration	10	0.0000125	± 0.0064	meters/sec^2
Y_G Acceleration	10	0.0000125	± 0.0064	meters/sec^2
Z_G Acceleration	10	0.0000625	± 0.032	meters/sec^2
a_{Gf0}	12	2^{-31}	$\pm 0.9537\times10^{-6}$	seconds
a_{Gf1}	8	2^{-40}	$\pm 1.1642\times10^{-10}$	seconds/sec

Figure 4: Type 9 GEO ephemeris parameters [4]

Based on this broadcast information, the position vector of the satellite in ECEF coordinates is computed using the following kinematic relationship:

$$\mathbf{r}(t) = \begin{bmatrix} x_G \\ y_G \\ z_G \end{bmatrix} + \begin{bmatrix} \dot{x}_G \\ \dot{y}_G \\ \dot{z}_G \end{bmatrix}(t-t_0) + \frac{1}{2}\begin{bmatrix} \ddot{x}_G \\ \ddot{y}_G \\ \ddot{z}_G \end{bmatrix}(t-t_0)^2 \qquad (1)$$

This format was intended for use with truly geostationary satellites. It thus has limited dynamic range on the component of position perpendicular to the equatorial plane, namely, the ECEF z-component. This is problematic even for satellites which are very nearly in GEO. A primary example of this is the European SBAS satellite, Artemis. Artemis is a European Space Agency (ESA) telecommunications satellite which, as part of its duty, acts as a satellite in the European Geostationary Navigation Overlay Service (EGNOS). During orbital insertion, the Ariane 5 launch vehicle experienced a problem which resulted in Artemis being placed in a lower orbit than desired. Some clever engineering saved the satellite and placed it in nearly the required orbit, though this left the spacecraft low on fuel for orbit maintenance and station-keeping. The result is that Artemis is now in a GSO which is inclined to over 10 degrees with respect to the equator. This is enough to put the satellite outside of the dynamic range of the current MT 9 ECEF z-component (Figure 4) during certain parts of its orbit and thus cannot be used for ranging. This is shown by the simple calculation in Figure 5 and demonstrates the limitations of the current MOPS ephemeris.

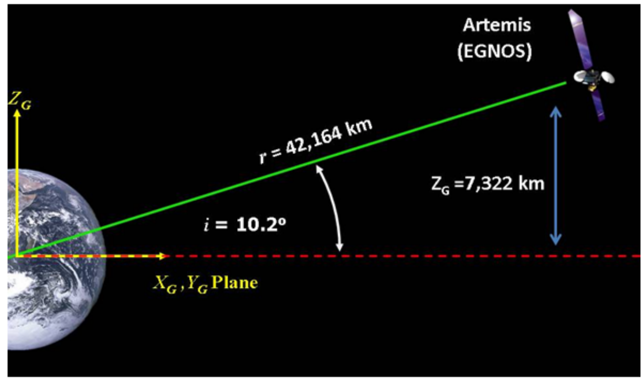

Figure 5: Artemis out-of-plane motion

Almanac

The current MOPS GEO almanac message (MT 17) is a low resolution message which is meant to be used by the receiver in satellite acquisition. This message is valid for a period of weeks and is typically accurate to within a few degrees in terms of solid angle. This tells the receiver whether or not the particular satellite is expected to be in view and whether it should spend effort searching for it. The almanac message format is given in Figure 6 below.

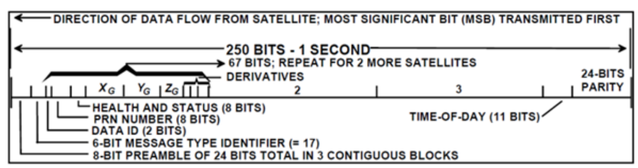

Figure 6: Type 17 GEO almanac message format [4]

Parameter	No. of Bits (Note 1)	Scale Factor (LSB)	Effective Range (Note 1)	Units
For each of 3 satellites	67	—	—	—
Data ID	2	1	0 to 3	unitless
PRN Number	8	1	0 to 210	—
Health and Status	8	—	—	unitless
X_G (ECEF)	15	2,600	±42,595,800	meters
Y_G (ECEF)	15	2,600	±42,595,800	meters
Z_G (ECEF)	9	26,000	±6,630,000	meters
X_G Rate-of-Change	3	10	± 40	meters/sec
Y_G Rate-of-Change	3	10	± 40	meters/sec
Z_G Rate-of-Change	4	60	± 480	meters/sec
t_0 (Time-of-Day)	11	64	0 to 86,336	seconds

Figure 7: Type 17 GEO almanac parameters [4]

The almanac message makes use of 6 parameters to calculate the satellite position, namely the ECEF position and velocity. The satellite position is calculated via the following kinematic relationship:

$$\mathbf{r}(t) = \begin{bmatrix} x_G \\ y_G \\ z_G \end{bmatrix} + \begin{bmatrix} \dot{x}_G \\ \dot{y}_G \\ \dot{z}_G \end{bmatrix}(t-t_0) \qquad (2)$$

Like the ephemeris message, this message was again intended for use with only GEO satellites and also has limitations in dynamic range of the component of position outside the equatorial plane (Figure 7). This again leads to limitations on existing SBAS satellites such as Artemis.

PROPOSED MOPS MESSAGE

The future of GNSS will involve many different orbital regimes and thus developing a message to support all of them will allow for the MOPS message to be delivered by satellites in a variety of different orbits, not just those in GEO. To describe the position of these different satellites with a single message requires that we look towards a more general orbit description.

The most basic general orbit description is the so-called classical orbital elements which consist of 6 parameters that describe the state of a satellite at a given epoch. This simple model assumes that spacecraft in closed orbits follow an elliptical path fixed in inertial space. The shape of the trajectory is given by the eccentricity e of the ellipse. The size is given by the semi-major axis a, and is half the length of the long axis of the ellipse. Three Euler angles are used to describe the orientation of the ellipse in inertial space. The inclination i is the angle of the orbital plane with respect the equator, the right ascension of the ascending node Ω is the angle measured in the equatorial plane between the vernal equinox and the and the point of right ascension, and the argument of perigee ω is the angle measured in the orbital plane between the right ascension crossing and the point of closest approach on the Earth. The last parameter is the mean anomaly M_0 which describes the position of the satellite in the orbital plane at epoch. More detail on these parameters can be found in [5].

These six parameters are not sufficiently accurate to describe satellite motion to the desired centimeter level. The reason for this is that the motion is more complex is due to the various perturbation forces that act on the spacecraft. The simplified model assumes that the spacecraft orbits a perfectly uniform and spherical Earth. In reality, the Earth has a non-uniform mass distribution, the dominant deviation being a bulge at the equator. This J_2 spherical harmonic term causes precession of the orbital plane and higher order gravity terms cause more complex deviations. The Sun and Moon also pull on the satellite with their respective gravity fields. The Earth's atmosphere causes a drag force on the satellite which dissipates energy. Lastly, as the Sun's rays reflect off the satellite, it gets pushed in the other direction. This solar radiation pressure is caused by photons exchanging momentum with the satellite. All of these effects combined give rise to a more complex trajectory and require more parameters for an accurate description.

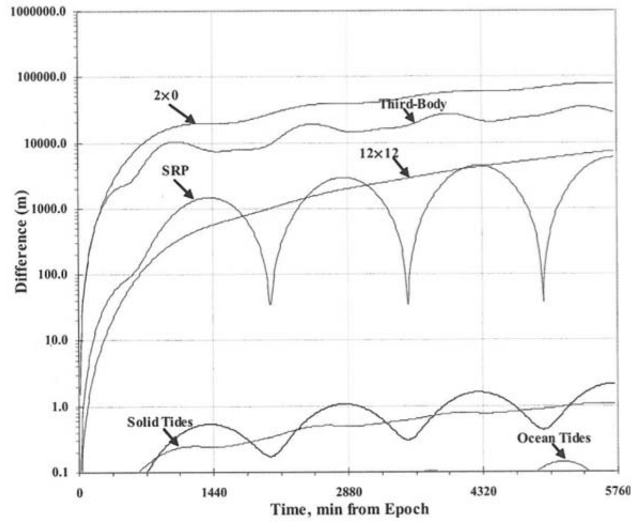

Figure 8: Typical perturbations in GEO [5]

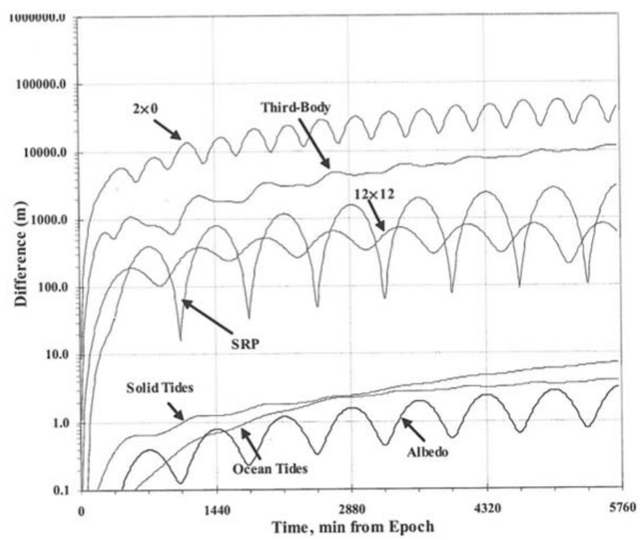

Figure 9: Typical perturbations in MEO [5]

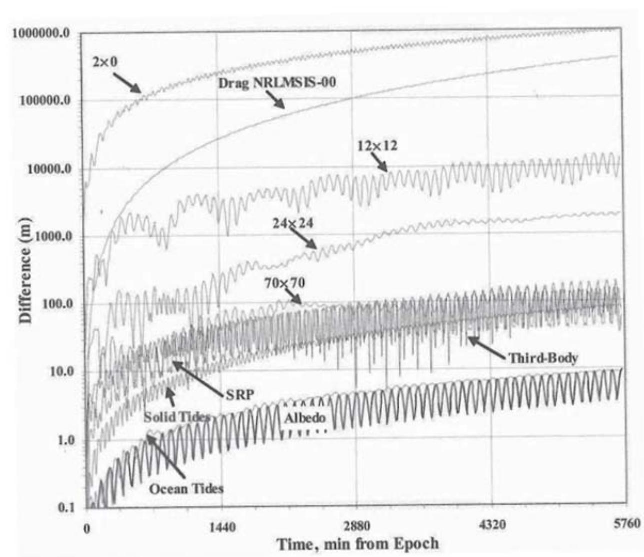

Figure 10: Typical perturbations in LEO [5]

The relative magnitudes of the different perturbation forces in GSO, MEO, and LEO are given in Figures 8, 9, and 10 respectively. These plots demonstrate the loss of accuracy obtained by neglecting a particular perturbation in a high precision orbit propagator.

In order to capture these effects, an augmented set of orbital elements must be employed. GPS makes use of an augmented set of 15 orbital elements in its ephemeris message to achieve the necessary accuracy [6]. A summary table of these elements and their function is given in Table 1. These additional elements capture more of the physics which causes deviation from a perfect ellipse. There are 9 additional elements in the GPS ephemeris. The 6 harmonic correction terms account for the Earth's oblate shape and resulting gravity field. Rates in the inclination IDOT and right ascension $\dot{\Omega}$ account for precession of the orbital plane. This effect is due in part to J_2 but also from other combined perturbation effects. The remaining element, a correction to the satellite's mean orbital rate Δn, is again due to combined effects.

Parameter	Description
M_0	Mean Anomaly at Reference Time
Δn	Mean Motion Correction
e	Eccentricity
a	Semi-Major Axis
Ω_0	Right Ascension of Ascending Node at Epoch
i_0	Inclination at Epoch
ω	Argument of Perigee
$\dot{\Omega}$	Rate of Right Ascension
IDOT	Rate of Inclination
C_{uc}	Amplitude of Cosine Correction Term to Argument of Latitude
C_{us}	Amplitude of Sine Correction Term to Argument of Latitude
C_{rc}	Amplitude of Cosine Correction Term to Orbit Radius
C_{rs}	Amplitude of Sine Correction Term to Orbit Radius
C_{ic}	Amplitude of Cosine Correction Term to Inclination
C_{ic}	Amplitude of Sine Correction Term to Orbit Radius

Table 1: GPS Ephemeris Orbital Elements [6]

Ephemeris

The GPS ephemeris orbital elements must be valid for up to 4 hours, however, for the MOPS we only require 10 minutes and thus a subset of these elements is sufficient. Working within the GPS ephemeris orbital elements has the added benefit of existing user algorithms for computing satellite ECEF positions based on orbital elements. A subset of 9 of these elements proved enough for orbits in MEO and GSO but only offers limited capacity in LEO. The goal here was to provide support primarily for MEO and GSO, some usability in LEO is seen here as an added bonus. The current Type 9 message makes use of 9 pieces of information, thus, we have maintained the same number of degrees-of-freedom in this new message. The orbital elements selected were the semi-major axis a, eccentricity e, inclination at epoch i_0, rate in inclination IDOT, right ascension at epoch Ω_0, argument of perigee ω, and the along-track harmonic correction terms C_{us} and C_{uc}. The proposed L5 MOPS message allows for the satellite positioning information to be broken into 2 messages [1], the proposed message structure is shown in Figure 11 and message details such as bit allocation, scale factors, and dynamic ranges are given in Table 2.

Parameter	No. of Bits	Scale Factor (LSB)	Effective Range	Units
PRN	8	1	1 – 210	-
IODG × 2	8	1	0 – 16	-
Health & Status	3	-	-	-
Provider ID	4	-	-	-
a	32	0.01	$0 - 4.29\times10^{7}$	meters
e	31	2^{-31}	0 – 1	-
i_0	34	$\pi \times 2^{-34}$	$0 - \pi/2$	radians
Ω_0	35*	$\pi \times 2^{-34}$	$\pm \pi$	radians
Ω	35*	$\pi \times 2^{-34}$	$\pm \pi$	radians
M_0	35*	$\pi \times 2^{-34}$	$\pm \pi$	radians
IDOT	22*	8.5×10^{-14}	$\pm1.78\times10^{-14}$	rad/sec
C_{uc}	22*	6.5×10^{-10}	±0.0014	radians
C_{us}	22*	6.5×10^{-10}	±0.0014	radians
Time of day, t_0	13	16	0 - 86,384	seconds
a_{Gf0}	12*	0.02	±40.96	meters
a_{Gf1}	10*	5×10^{-5}	±0.0256	m/sec
Scale Exponent	3	1	0 – 7	-
$E_{1,1}$	9	1	0 – 511	-
$E_{2,2}$	9	1	0 – 511	-
$E_{3,3}$	9	1	0 – 511	-
$E_{4,4}$	9	1	0 – 511	-
$E_{1,2}$	10*	1	± 512	-
$E_{1,3}$	10*	1	± 512	-
$E_{1,4}$	10*	1	± 512	-
$E_{2,3}$	10*	1	± 512	-
$E_{2,4}$	10*	1	± 512	-
$E_{3,4}$	10*	1	± 512	-
DFREI	4	1	0 – 15	-

*signed value coded as two's compliment

Table 2: The L5 SBAS satellite ephemeris message

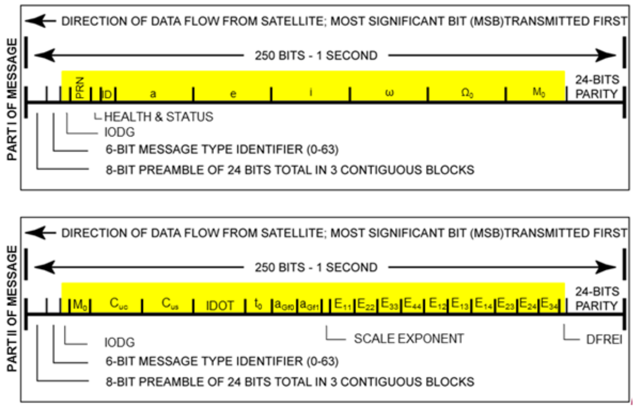

Figure 11: The L5 SBAS satellite ephemeris message format

Almanac

The almanac message chosen also works within the set of GPS orbital elements, in this case a subset of 7. In fact, those which were determined to work best for satellites in MEO and GSO were those used by the GPS almanac, namely, the semi-major axis a, eccentricity e, inclination i, right ascension Ω_0, argument of perigee ω, mean anomaly M_0, as well as the rate in the right ascension $\dot{\Omega}$. With this format, two almanac messages can fit into a single message block as shown in Figure 12. The message details, such as bit allocation, scale factors, and dynamic ranges are given in Table 3. This scheme does not work well with satellites in LEO. The fundamental difficulty is that these satellites are moving very quickly and are thus in view to a receiver on the order of 10 minutes. In addition to this, perturbations in GSO and MEO are of a similar order, whereas those in LEO are closer to a factor of 10 stronger than either of these two cases (see Figures 8-10).

Parameter	No. of Bits	Scale Factor (LSB)	Effective Range	Units
PRN	8	1	1 – 210	-
Health & Status	3	-	-	-
Provider ID	4	-	-	-
a	17	500	$0 – 6.55\times10^{7}$	Meters
e	8	2^{-8}	0 – 1	-
i_0	13	$\pi \times 2^{-13}$	0 - π/2	radians
Ω_0	14*	$\pi \times 2^{-13}$	± π	radians
$\dot{\Omega}$	8*	10^{-9}	$\pm 1.28\times10^{-7}$	rad/sec
ω	15*	$\pi \times 2^{-14}$	± π	radians
M_0	15*	$\pi \times 2^{-14}$	± π	radians
Time of day, t_0	6	1800	0 - 84,600	seconds

*signed value coded as two's compliment

Table 3: The L5 SBAS satellite almanac message

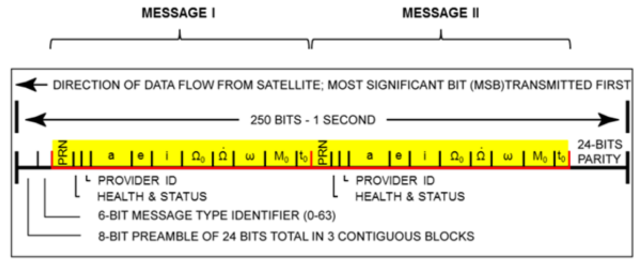

Figure 12: The L5 SBAS satellite almanac message format

FITTING OF ORBITAL ELEMENTS

High precision orbit propagators are used to predict the trajectories of GNSS and SBAS spacecraft. This information is then packaged into orbital elements in the form of Figure 3 and distributed to the user. The method used to fit orbital elements to the propagated dataset is the subject of this section.

This problem amounts to a nonlinear optimization problem. We wish to fit the orbital elements to the propagated high fidelity dataset in a way which minimizes position errors at all time steps for the interval in question. This yields the best possible resolution of the data to the user. The derivation given here is for the 9 orbital element ephemeris message though the methods developed are general and can be used with other orbital elements than the ones chosen.

The position of a satellite $\mathbf{r}(t)$ is assumed to be a function of the orbital elements $\mathbf{x}$ and time t where:

$$\mathbf{x} = \left[a, e, i, \Omega, \omega, M_0, \mathrm{IDOT}, C_{us}, C_{uc}\right]^T \tag{3}$$

So we can write the position vector at time t as:

$$\mathbf{r}(t) = \mathbf{f}(\mathbf{x}, t) \tag{4}$$

For the case of 9 orbital elements, this function is the following algorithm:

1. Compute the mean orbital rate n:

$$n = \sqrt{\frac{\mu}{a^3}} \tag{5}$$

   where a is the semi-major axis and μ is the gravitational parameter of the Earth.

2. Compute the mean anomaly:

$$M = M_0 + n\left(t - t_0\right) \tag{6}$$

   where M_0 is the mean anomaly at epoch t_0.

3. Compute the eccentric anomaly E by solving Kepler's Equation:

$$M = E - e \sin E \tag{7}$$

where e is the eccentricity.

4. Compute the true anomaly:

$$\nu = \operatorname{atan2}\left(\sqrt{1-e^2}\sin E, \cos E - e\right) \tag{8}$$

5. Compute the orbit radius:

$$r = \frac{a\,(1-e^2)}{1+e\cos\nu} \tag{9}$$

6. Compute the inclination:

$$i = i_0 + \mathrm{IDOT}\left(t - t_0\right) \tag{10}$$

7. Compute the argument of latitude:

$$\Phi = \nu + \omega \tag{11}$$

$$\delta u = C_{us}\sin 2\Phi + C_{uc}\cos 2\Phi \tag{12}$$

$$u = \Phi + \delta u \tag{13}$$

8. Compute the Earth Centered Inertial (ECI) position vector of the satellite:

$$\mathbf{r}(t) = r\begin{bmatrix} \mathrm{c}_u\mathrm{c}_\Omega - \mathrm{s}_u\mathrm{c}_i\mathrm{s}_\Omega \\ \mathrm{c}_u\mathrm{s}_\Omega + \mathrm{s}_u\mathrm{c}_i\mathrm{c}_\Omega \\ \mathrm{s}_u\mathrm{s}_i \end{bmatrix} \tag{14}$$

where c_α and s_α are $\cos\alpha$ and $\sin\alpha$, respectively.

The orbit fitting scheme discussed here fits the orbit in ECI coordinates, though the final desired position is in ECEF coordinates. This is achieved with the following last step:

9. Compute the longitude of the ascending node with respect to the ECEF coordinate system Ω_l:

$$\Omega_l = \Omega - \{\theta_{ref} + \Omega_e(t - t_{ref})\} \tag{15}$$

where Ω is the right ascension angle, Ω_e is the rotation rate of the Earth, and θ_{ref} is the so-called sidereal time at the reference time t_{ref}. The ECI and ECEF coordinate frames share the same z-axis. They differ by a rotation about this axis through an angle equal to the sidereal time. The position in ECEF coordinates is then given by:

$$\mathbf{r}(t) = r\begin{bmatrix} \mathrm{c}_u\mathrm{c}_{\Omega_l} - \mathrm{s}_u\mathrm{c}_i\mathrm{s}_{\Omega_l} \\ \mathrm{c}_u\mathrm{s}_{\Omega_l} + \mathrm{s}_u\mathrm{c}_i\mathrm{c}_{\Omega_l} \\ \mathrm{s}_u\mathrm{s}_i \end{bmatrix} \tag{16}$$

The orbital element model does capture most of the physics of the motion. We thus expect the orbital elements to vary only in a small amount with time relative to some nominal parameters. Thus, we can linearize this nonlinear function by keeping the linear term of a Taylor Expansion about a nominal set of orbital elements **p** and obtain a decent approximation:

$$\mathbf{r}(t) \approx \mathbf{f}(\mathbf{p},t) + \frac{\partial \mathbf{f}}{\partial \mathbf{x}}\cdot\left(\mathbf{x}-\mathbf{p}\right) \tag{17}$$

where here the partial derivative of the function **f** with respect to the orbital elements **x** is the Jacobian matrix **J**:

$$\mathbf{J} \equiv \frac{\partial \mathbf{f}}{\partial \mathbf{x}} \tag{18}$$

Written explicitly, the Jacobian matrix is:

$$\mathbf{J} = \left[\frac{\partial \mathbf{f}}{\partial a}\ \frac{\partial \mathbf{f}}{\partial e}\ \frac{\partial \mathbf{f}}{\partial i}\ \frac{\partial \mathbf{f}}{\partial \Omega}\ \frac{\partial \mathbf{f}}{\partial \omega}\ \frac{\partial \mathbf{f}}{\partial M_0}\ \frac{\partial \mathbf{f}}{\partial \mathrm{IDOT}}\ \frac{\partial \mathbf{f}}{\partial C_{us}}\ \frac{\partial \mathbf{f}}{\partial C_{uc}}\right] \tag{19}$$

These partial derivatives are as follows:

$$\frac{\partial \mathbf{f}}{\partial a} = \frac{1}{a}\mathbf{f}(\mathbf{p},t) \tag{20}$$

$$\frac{\partial \mathbf{f}}{\partial e} = -\left(\frac{\cos\nu + e^2\cos\nu + 2e}{(1-e^2)(1+e\cos\nu)}\right)\mathbf{f}(\mathbf{p},t) \tag{21}$$

$$\frac{\partial \mathbf{f}}{\partial i} = r\begin{bmatrix} \mathrm{s}_u\mathrm{s}_i\mathrm{s}_\Omega \\ -\mathrm{s}_u\mathrm{s}_i\mathrm{c}_\Omega \\ \mathrm{s}_u\mathrm{c}_i \end{bmatrix} \tag{22}$$

$$\frac{\partial \mathbf{f}}{\partial \mathrm{IDOT}} = \frac{\partial \mathbf{f}}{\partial i}\cdot(t - t_0) \tag{23}$$

$$\frac{\partial \mathbf{f}}{\partial \Omega} = r\begin{bmatrix} -\mathrm{c}_u\mathrm{s}_\Omega - \mathrm{s}_u\mathrm{c}_i\mathrm{c}_\Omega \\ \mathrm{c}_u\mathrm{c}_\Omega - \mathrm{s}_u\mathrm{c}_i\mathrm{s}_\Omega \\ 0 \end{bmatrix} \tag{24}$$

$$\frac{\partial \mathbf{f}}{\partial \omega} = r\begin{bmatrix} -\mathrm{s}_u\mathrm{c}_\Omega - \mathrm{c}_u\mathrm{c}_i\mathrm{s}_\Omega \\ -\mathrm{s}_u\mathrm{s}_\Omega + \mathrm{c}_u\mathrm{c}_i\mathrm{c}_\Omega \\ \mathrm{c}_u\mathrm{s}_i \end{bmatrix}\left(1 + \frac{\partial \delta u}{\partial u}\right) \tag{25}$$

where:

$$\frac{\partial \delta u}{\partial u} = 2\left[C_{us}\cos 2\Phi - C_{uc}\sin 2\Phi\right] \tag{26}$$

Those for the harmonic correction terms are:

$$\frac{\partial \mathbf{f}}{\partial C_{uc}} = r\cos 2\Phi \begin{bmatrix} -\mathrm{s}_u\mathrm{c}_\Omega - \mathrm{c}_u\mathrm{c}_i\mathrm{s}_\Omega \\ -\mathrm{s}_u\mathrm{s}_\Omega + \mathrm{c}_u\mathrm{c}_i\mathrm{c}_\Omega \\ \mathrm{c}_u\mathrm{s}_i \end{bmatrix} \tag{27}$$

$$\frac{\partial \mathbf{f}}{\partial C_{us}} = r\sin 2\Phi \begin{bmatrix} -\mathrm{s}_u\mathrm{c}_\Omega - \mathrm{c}_u\mathrm{c}_i\mathrm{s}_\Omega \\ -\mathrm{s}_u\mathrm{s}_\Omega + \mathrm{c}_u\mathrm{c}_i\mathrm{c}_\Omega \\ \mathrm{c}_u\mathrm{s}_i \end{bmatrix} \tag{28}$$

The last partial derivative, that with respect to the mean anomaly M_0, requires a little more attention. This can be written as the product of 3 partial derivatives.

$$\frac{\partial \mathbf{f}}{\partial M_0} = \underbrace{\frac{\partial \mathbf{f}}{\partial \nu}}_{I}\underbrace{\frac{\partial \nu}{\partial E}}_{II}\underbrace{\frac{\partial E}{\partial M_0}}_{III} \tag{29}$$

For I, the partial derivative is given by:

$$\frac{\partial \mathbf{f}}{\partial \nu} = \frac{\partial \mathbf{f}}{\partial \omega} + \frac{e\sin\nu}{1+e\cos\nu}\mathbf{f}(\mathbf{p},t) \tag{30}$$

For II, we will make use of use of the following relationship between true anomaly and eccentric anomaly [7]:

$$\tan\frac{\nu}{2} = \sqrt{\frac{1+e}{1-e}}\tan\frac{E}{2} \tag{31}$$

Solving for ν and taking the partial derivative with respect to E results in:

$$\frac{\partial \nu}{\partial E} = \frac{2\sqrt{\frac{1+e}{1-e}}}{1+\cos E + \frac{1+e}{1-e}\left(1-\cos E\right)} \tag{32}$$

For III, we will make use of Kepler's Equation in the form:

$$M_0 = E - e\sin E - n\left(t - t_0\right) \tag{33}$$

Taking the partial derivative with respect to E results in:

$$\frac{\partial M_0}{\partial E} = 1 - e\cos E \tag{34}$$

We can now find the desired partial derivative using the following relationship:

$$\frac{\partial E}{\partial M_0} = \left(\frac{\partial M_0}{\partial E}\right)^{-1} = \frac{1}{1-e\cos E} \tag{35}$$

Now, to solve for the optimal orbital elements. We have computed the position $\mathbf{r}(t)$ using a precision orbit propagator at discrete times t_i. We can linearize about the first epoch and take $\mathbf{p}$ to be the orbital elements at time t_0. This gives us an approximation at each time step of the form:

$$\mathbf{r}(t_i) \approx \mathbf{f}(\mathbf{p},t_i) + \mathbf{J}\,\boldsymbol{\delta}\mathbf{x} \tag{36}$$

where $\boldsymbol{\delta}\mathbf{x} \equiv \mathbf{x} - \mathbf{p}$. Taking the above as an equality, we can stack these N discrete points to form the following system of equations:

$$\mathbf{J}\,\boldsymbol{\delta}\mathbf{x} = \begin{bmatrix} \mathbf{r}(t_0) \\ \mathbf{r}(t_1) \\ \vdots \\ \mathbf{r}(t_{N-1}) \end{bmatrix} - \begin{bmatrix} \mathbf{f}(\mathbf{p},t_0) \\ \mathbf{f}(\mathbf{p},t_1) \\ \vdots \\ \mathbf{f}(\mathbf{p},t_{N-1}) \end{bmatrix} \tag{37}$$

The above now has the form of an over determined linear system $\mathbf{A}\mathbf{y} = \mathbf{b}$. We can obtain a least squares approximation to $\mathbf{y}$ via the Moore-Penrose pseudo-inverse [8]:

$$\mathbf{y} = \mathbf{A}^{\dagger}\mathbf{b} = (\mathbf{A}^T\mathbf{A})^{-1}\mathbf{A}\,\mathbf{b} \tag{38}$$

This allows us to solve for the difference between the actual orbital elements and those we linearized around:

$$\boldsymbol{\delta}\mathbf{x} = \mathbf{J}^{\dagger}\left(\begin{bmatrix} \mathbf{r}(t_0) \\ \mathbf{r}(t_1) \\ \vdots \\ \mathbf{r}(t_{N-1}) \end{bmatrix} - \begin{bmatrix} \mathbf{f}(\mathbf{p},t_0) \\ \mathbf{f}(\mathbf{p},t_1) \\ \vdots \\ \mathbf{f}(\mathbf{p},t_{N-1}) \end{bmatrix}\right) \tag{39}$$

This result is not the final answer. This result must be iterated upon in order to obtain the optimal result. The obtained $\boldsymbol{\delta}\mathbf{x}$ is a successive update in an iterative scheme:

$$\mathbf{p} = \mathbf{p} + \boldsymbol{\delta}\mathbf{x} \tag{40}$$

After a sufficient number of iterations (typically 10), $\boldsymbol{\delta}\mathbf{x}$ approaches zero and $\mathbf{p}$ approaches the optimal set of orbital elements $\mathbf{p}^{\star}$.

RESULTS

In this section, the results for certain orbit classes are given in order to showcase the capability of the fitting algorithm and the effectiveness of the proposed L5 ephemeris and almanac messages.

In order to perform this analysis, several high fidelity orbit trajectories were required. These are widely available for spacecraft such as GPS but not for others such as satellites in LEO or Moniya type orbits. Our solution was to use the commercial software package

Satellite Tool Kit (STK) by Analytical Graphics Inc. (AGI) to generate these datasets. This software has a large library of satellites based on the NORAD Two Line Element (TLE) sets. STK has built in high precision orbit propagators which were used in this analysis to generate the required high fidelity trajectories.

The scheme used for orbital element fitting in both the ephemeris and almanac case was that outlined in the previous section, where the high fidelity trajectory is obtained via STK. A block diagram of the overall scheme is given in Figure 13.

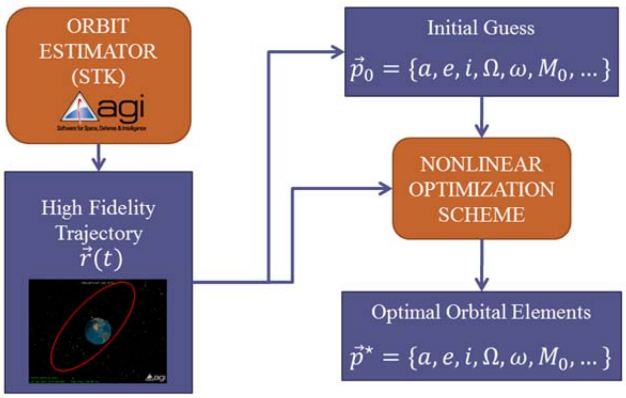

Figure 13: Orbital element fitting scheme

Orbits

In this section, a brief discussion of the orbits chosen for analysis, their unique properties, and their reason for selection will be discussed. A summary of the satellites used and their properties is given in Table 4.

Satellite	Orbit Class	Period [sidereal days]	Eccen.	Incl. [deg]
CRW	GEO	1	~ 0	~ 0
Artemis	IGSO	1	~ 0	10.2
BeiDou	IGSO	1	~ 0	55
QZSS	IGSO	1	0.075	40
GPS	MEO	1/2	~ 0	55
GLONASS	MEO	8/17	~ 0	63.4
Molniya	HEO	1/2	0.75	63.4
Iridium	LEO	0.07	~ 0	87

Table 4: Summary of orbits used for analysis

The first satellite chosen was one the existing SBAS GEOs, namely, the WAAS CRW. Its groundtrack, shown in Figure 14, demonstrates that this is truly a GEO satellite as it is always over the same point on the Earth. This spacecraft has a near zero inclination and is very nearly circular. Next is the Artemis satellite, that which breaks the limits of the current MT 9 MOPS message. This spacecraft is very nearly in a GEO orbit, though from its groundtrack it is clear that it is in a very slightly inclined orbit, about 10.2 degrees (see Figure 15). Moving to higher inclination orbits, the BeiDou IGSO-4 is an example of a circular IGSO at a 55 degree inclination (see Figure 16). QZS-1, the first satellite in the Japanese Quasi-Zenith Satellite System (QZSS), is an example of an eccentric IGSO. This satellite is at a 40 degree inclination and has an eccentricity of 0.075. This slight eccentricity gives rise to the special property that the satellite travels more slowly in the northern hemisphere (near apogee) and more quickly in the southern hemisphere (near perigee). This shows up in the lopsided groundtrack shown in Figure 17. This was by design, as the Japanese wanted a satellite that would linger at high elevations over Japan, not give coverage to the southern hemisphere.

Moving to MEO, both a GPS and a GLONASS satellite were chosen for analysis. GPS satellites are in near circular orbits with an inclination of 55 degrees. Their period of half a sidereal day gives rise to the repeating groundtrack shown in Figure 18. This orbit is similar in many respects to those of the MEO Galileo and BeiDou satellites. These satellites are both in near circular orbits with 55 degree inclinations, though their orbital periods vary slightly due to European and Chinese systems operating slightly higher altitudes. GLONASS is in a slightly different orbit than these other systems. It is also in a near circular orbit, though it is inclined to a higher 63.4 degrees, a value chosen for the J_2 invariant properties of the orbit. In addition, it is at a lower altitude than GPS making it slightly more susceptible to higher order gravity terms. Its orbital period is 8/17 sidereal days, meaning its groundtrack (see Figure 19) will repeat every 8 sidereal days.

Another orbit of special interest is the Molniya orbit. Like GPS, Molniya satellites have a repeat groundtrack, though these orbits are highly eccentric (HEO). These satellites were originally designed for telecommunications in high latitude regions of the Soviet Union. Like GLONASS, they are inclined to 63.4 degree in part to provide coverage at high latitudes but also to make use of the J_2 invariant properties of the orbit. It's high eccentricity of 0.75 gives the satellite the special property of spending majority of its time over the northern hemisphere. This can be seen from the groundtrack shown in Figure 20 where it moves quickly with respect to the Earth in the southern hemisphere and then moves more slowly than the Earth and falls behind in the north. There has been interest in using this type of orbit as a method for delivering integrity to Polar Regions where there is no coverage from GEO satellites [3].

Lastly, a LEO satellite from the Iridium constellation was selected for analysis. Consisting of 66 satellites in 6 orbital planes, this constellation is best known for its satellite phone service, providing coverage over the entire globe. More recently, it also has been examined a candidate for delivering both integrity and navigation services, for example [2]. These satellites are in an 800 km altitude near polar circular orbit and complete a revolution in about 100 minutes.

Figure 14: WAAS CRW groundtrack

Figure 15: EGNOS Artemis groundtrack

Figure 16: BeiDou IGSO 4 grountrack

Figure 17: QZS-1 groundtrack

Figure 18: GPS PRN 17 groundtrack

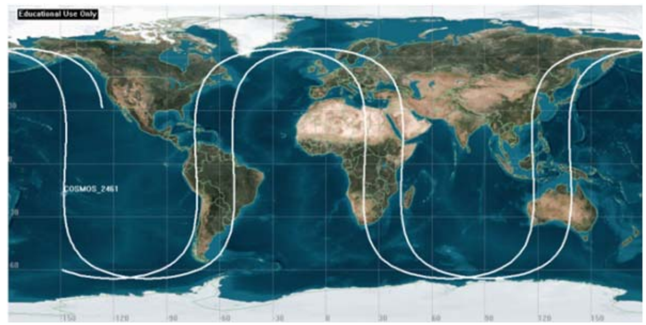

Figure 19: GLONASS Cosmos 2461 groundtrack

Figure 20: Molniya 3-53 groundtrack

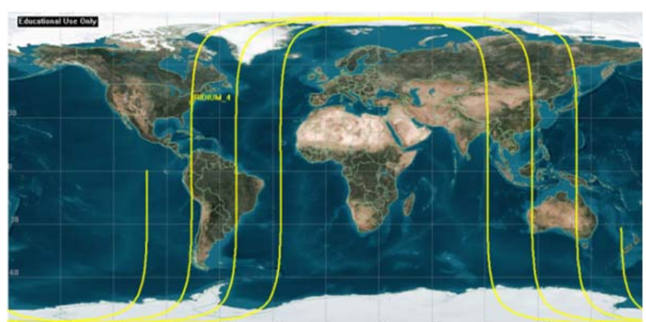

Figure 21: Iridium 4 groundtrack

Ephemeris

In this section we describe the results obtained for the L5 ephemeris message. For this message, we set a goal of a 3 cm satellite position resolution over a period of 10 minutes, a time interval which comes from the requirements given in [1]. What is meant by resolution in this context is that we want to represent the high fidelity orbit trajectory to within a 3D position of 3 cm. Thus, after fitting the orbital elements and quantizing via the scheme Table 2, we want to convey the high fidelity trajectory to the user to within 3 cm.

The first case considered was the WAAS CRW. Figure 22 shows the 3-D position resolution of the satellite with respect to the high fidelity STK dataset over the fit interval of 10 minutes. The collection of different lines represents different scenarios. To ensure consistency of the scheme, the orbit fit and quantization was performed every two hours over a given 24 hour period, hence the 12 lines on the plot. The result shows that the message consistently achieves the goal of 3 cm or better resolution for the SBAS GEO over the desired period of 10 minutes. Figure 23 shows the result obtained for the EGNOS Artemis satellite. This was the breaking point of the MOPS Type 9 message and the result shows that the scheme works comparably well for this case as is does for the GEO. The result for the higher inclination BeiDou IGSO-4 is given in Figure 24. As can be seen from the plot, it also meets our desired goals. Figure 25 shows that the scheme also meets the requirements for the more eccentric IGSO QZS-1.

Moving closer to the Earth into MEO, Figure 18 shows the result typical for a GPS satellite. This plot shows that the desired requirement is met, though the response is not as flat as it was for the GSOs. Here, we first notice that the fit appears to turn up at the edges, giving rise to a worse fit in these regions. This is an artifact of the fitting scheme used and end effects such as these are typical when fitting curves, even polynomials, to datasets. Second, there is a more noticeable, seemingly periodic curvature to the data. This is also present in the GSO case but is much smaller in amplitude and is smoothed out by the quantization process. The effect is also more noticeable in LEO (see Figure 29). It appears that as we move closer to the Earth, the unaccounted for higher order gravity effects become more present and noticeable. Another MEO satellite considered was the Cosmos 2461 GLONASS satellite. The results show that our desired resolution is met with the exception of the end points (see Figure 19). Another interesting observation is that the amplitude of the fit curve error is larger than that of GPS. This is as expected since the satellite is closed to the Earth and thus more susceptible to higher order gravity effects.

Like GPS and GLONASS, another 12 hour period orbit of interest is the highly eccentric (HEO) Molniya. The results in this case demonstrate that our target resolution is met with the exception of the end points (see Figure 28). The results shown for this Molniya orbit are for the northern hemisphere only, where the satellite is further from the Earth and theoretically in operation. The fitting algorithm struggles to achieve this resolution in the southern hemisphere where the satellite is very close to the Earth and is essentially in LEO. Thus, over the operational range of the satellite, the scheme appears to meet our requirements.

The final case is that of LEO, the results of which are given for the Iridium 29 satellite in Figure 29. In this case, a fit over the desired 10 minute interval proved to be insufficiently accurate as it was on the order of meters. Instead, a 2 minute interval was shown to yield a resolution of 15-20 centimeters which is of at least of some value to users. This 2 minute interval was chosen because the MOPS ephemeris is meant to be broadcast every 2 minutes and each message valid for 10 minutes. Special care would have to be taken with LEOs in this case. Figure 30 shows that if not updated, this 2 minute fit will grow to an inaccuracy of nearly half a kilometer by the end of the 10 minute interval.

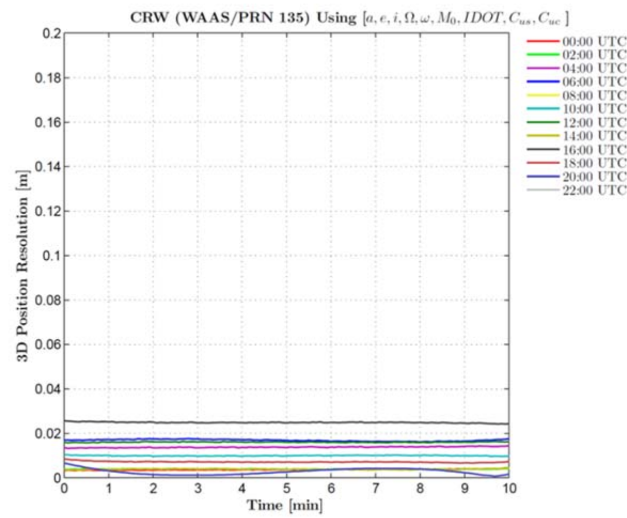

Figure 22: Results for WAAS CRW L5 ephemeris

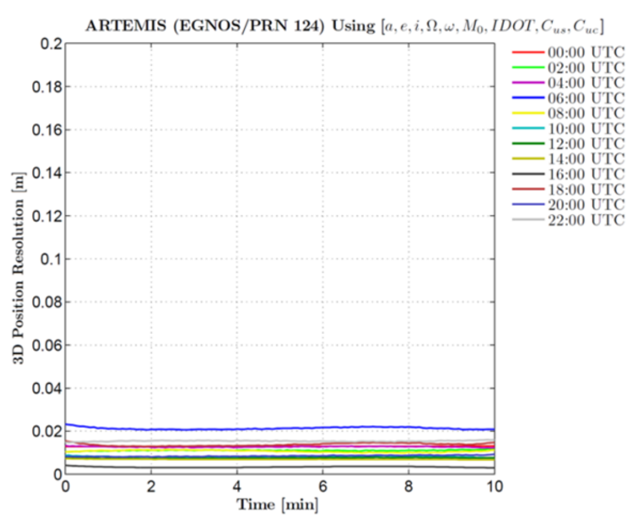

Figure 23: Results for EGNOS Artemis L5 ephemeris

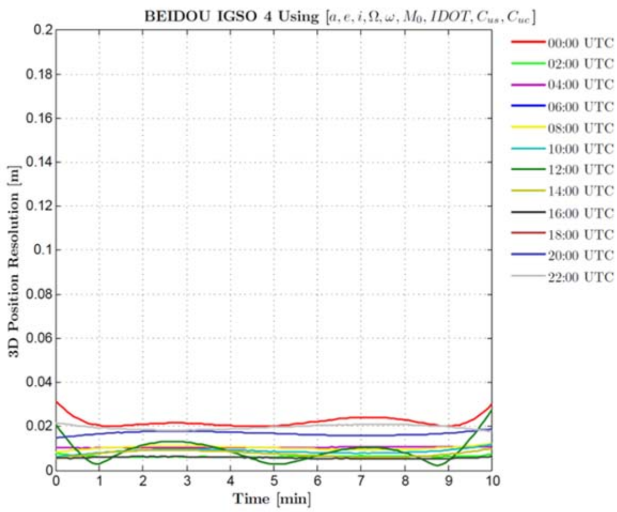

Figure 24: Results for BeiDou IGSO 4 L5 ephemeris

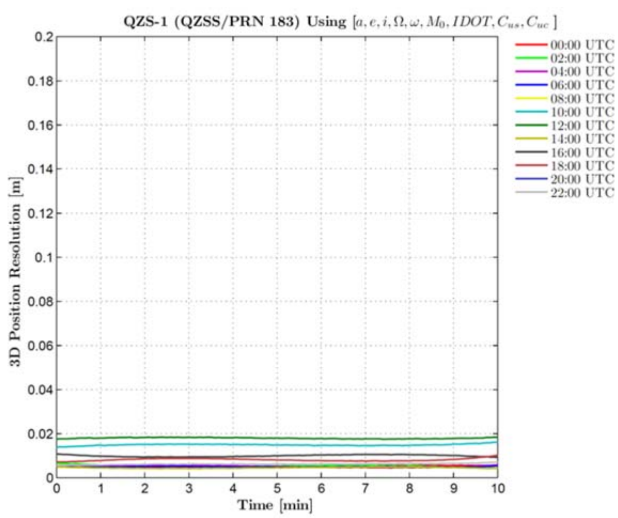

Figure 25: Results for QZS-1 L5 ephemeris

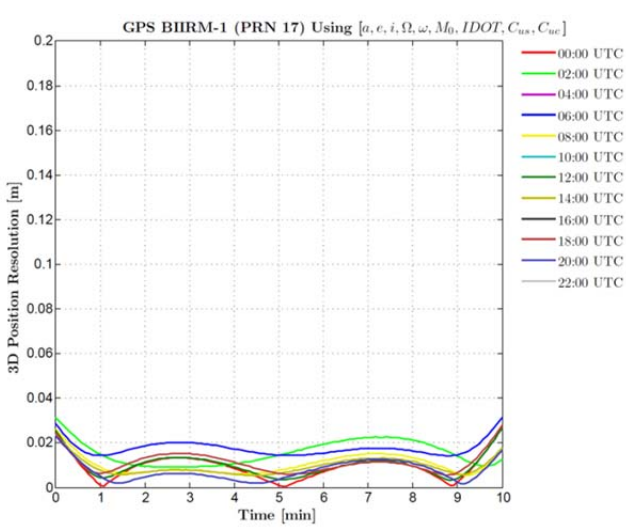

Figure 26: Results for GPS PRN 17 L5 ephemeris

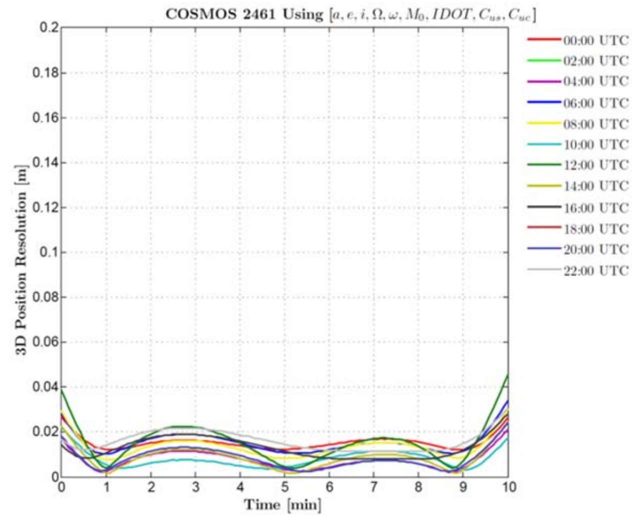

Figure 27: Results for GLONASS 735 L5 ephemeris

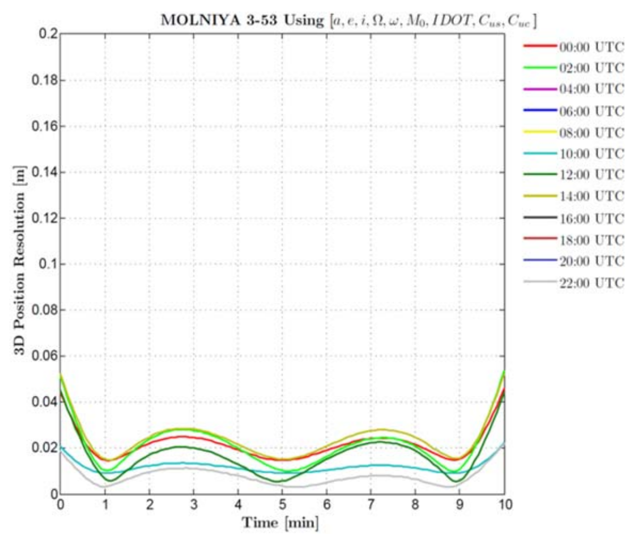

Figure 28: Results for Molniya 3-53 L5 ephemeris

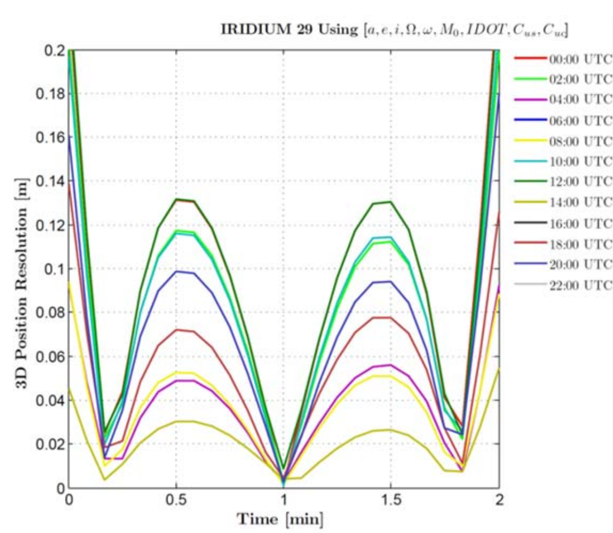

Figure 29: Results for Iridium 29 L5 ephemeris

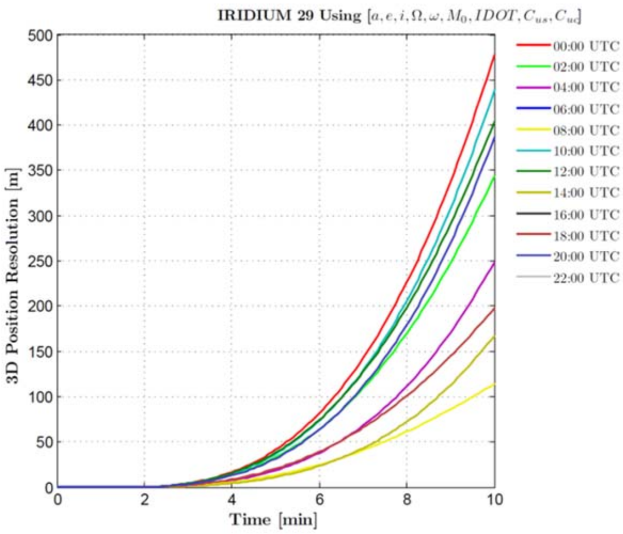

Figure 30: Results for Iridium 29 L5 ephemeris

Almanac

In this section we describe the results obtained for the L5 almanac message. For this message, a goal of 1 degree satellite position resolution in terms of solid angle over a period of several weeks was set. What is meant by resolution in this context is that we want to represent the high fidelity orbit trajectory to within a few degrees in the sky for an extended period of time. Thus, after fitting the orbital elements over a period of several weeks and quantizing via the scheme in Table 3, we want to have a dataset that can be stored and used by a receiver for use in determining whether a particular satellite is in view.

The first case considered was again the WAAS CRW. In this case a fitting interval of 60 days was used to produce the results shown in Figure 31. This plot shows the worst case angular position resolution over the satellite footprint after periods of 7, 14, 30, 60, 75, and 90 days. It demonstrates that the fit is sufficient to convey the satellite position to the receiver to within a worst case resolution of 2 degrees for up to 90 days. Although not shown here, this result is similar for both Artemis and the BeiDou IGSO. For QZS-1, a shorter fit interval of 35 days was used. This was chosen as the nonlinear fit scheme had some difficulties with convergence over longer periods of time. Figure 32 shows that over the fit interval, the angular resolution is less than 1 degree. Though it grows quickly to just under 4 degrees at the 90 day mark, it is still of value for use by the receiver.

In MEO, we again considered GPS and GLONASS. For both cases a fit interval of 30 days was found sufficient for long term resolution. Figure 33 shows that using this scheme, we can produce an angular resolution for GPS which is less than 1 degree over a period of 90 days. GLONASS does better still at less than half a degree over 90 days (see Figure 34). These results are expected for several reasons. First, it shows why these parameters were chosen for the GPS almanac as they clearly work well in capturing the physics of inclined MEO orbits. Second, MEO isn't hit as hard by quantization effects. In GSO, small errors in angular quantities due to quantization result in large position errors due to the further distance and hence longer lever arms of these orbits.

Lastly, we considered the Molniya orbit. Like QZSS, we experienced difficulties with fitting long intervals. As such, a two week interval was chosen, the results of which are shown in Figure 35. This shows that we can maintain a usable angular resolution of 1.5 degrees for up to 30 days. Although this is a usable result, it is interesting that orbits of higher eccentricity appear to be more difficult to fit. The speed at which this and the QZSS satellites drift in terms of angular position resolution compared to their more circular counterparts suggests that it is indeed the eccentricity that causes failure of the algorithm. This is not because of the value itself but because there is a larger drift in the orbital elements with time for these orbits.

In all of these cases, no orbit maintenance was taken into account. In other words, the satellite's most recent position was taken and propagated forward 90 days. In reality, some spacecraft have a station-keeping schedule which may be of the same order of some of the anticipated almanac validity intervals shown here. QZSS, for example, has maintenance scheduled approximately every 150 days [9]. Maintenance schedules can be built into orbit estimators but since schedules can change it may be more robust to alert users of satellites maintenance as it occurs. This would a valid almanac at all times. Interesting enough, if orbit maintenance schedules are known and orbital elements are actively being maintained then it may be easier to fit orbital elements for longer periods of time.

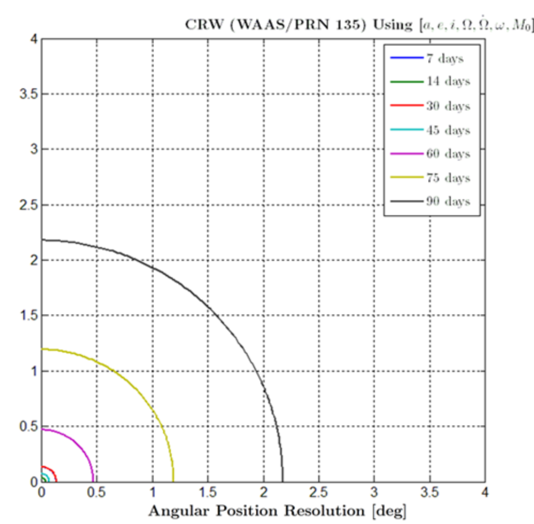

Figure 31: Results for WAAS CRW L5 almanac

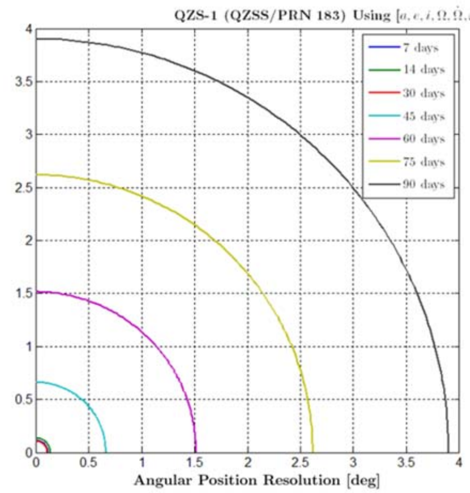

Figure 32: Results for QZS-1 L5 almanac

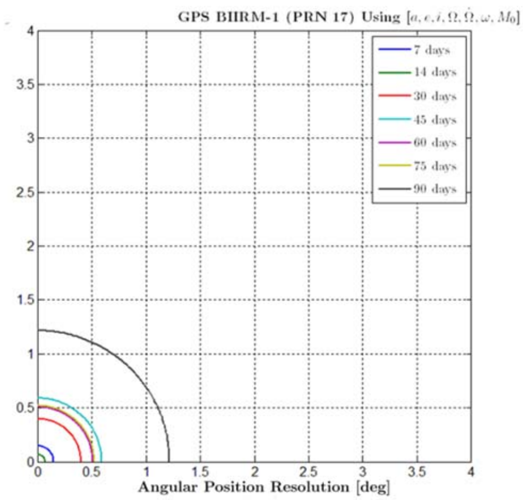

Figure 33: Results for GPS PRN 17 L5 almanac

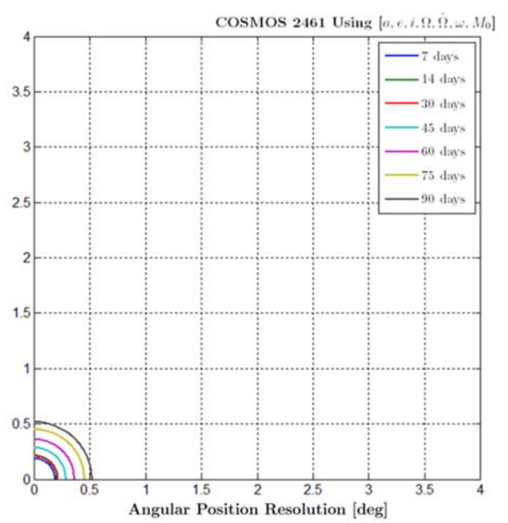

Figure 34: Results for GLONASS 735 L5 almanac

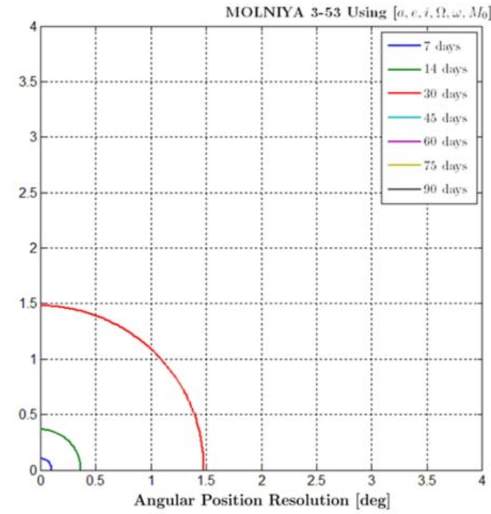

Figure 35: Results for Molniya 3-53 L5 almanac

CONCLUSION

In conclusion, an orbit fitting algorithm has been developed which is general in nature and can be used to fit a variety of orbital elements to a high fidelity satellite trajectory. This algorithm can be used for both short term and long term orbit fitting applications. Using this tool, candidates have been developed which could serve as the L5 MOPS ephemeris and almanac messages to support multiple orbit classes.

The L5 ephemeris message would be valid for an interval of 10 minutes and can delivery centimeter level resolution for satellites in GSO, MEO, and HEO orbits with limited capability in LEO. This message would come in two message blocks and would consist of 9 parameters, namely, the classical 6 Keplerian elements along with harmonic corrections in the along-track direction and a correction rate in inclination.

The L5 almanac message would be valid for use from 30-90 days by receivers in determining satellites in view. It is typically valid to 1 degrees in solid angle, 4 degrees in the worst case, for satellites in GSO, MEO, and HEO. Two messages would come in a single message block. The message consists of 7 parameters, namely, the classical 6 Keplerian elements along with a correction rate in the right ascension.

Though it takes more bits to convey the information for the L5 ephemeris and almanac compared to its L1 predecessor, the advantage is that a broader class of satellite orbits can be supported and thus more satellites can be considered for GNSS integrity applications in the future.

ACKNOWLEDGMENTS

The authors would like to gratefully acknowledge the FAA Satellite Product Team for supporting this work under Cooperative Agreement 2008-G-007. The opinions expressed in this paper are the author's and this paper does not represent a government position on the future development of L1/L5 WAAS.

REFERENCES

[1] T. Walter, J. Blanch and P. Enge, "L1/L5 SBAS MOPS to Support Multiple Constellations," in *Proceedings of the 25th International Technical Meeting of the Satellite Division of the Institute of Navigation (ION GNSS)*, Nashville, TN, 2012.

[2] G. X. Gao, L. Heng, T. Walter and P. Enge, "Breaking the Ice: Navigating in the Arctic," in *Proceedings of the 24th International Technical Meeting of the Satellite Division of the Institute of Navigation (ION GNSS)*, Portland, OR, 2011.

[3] T. Sundlisæter, T. Reid, C. Johnson and S. Wan, "GNSS and SBAS System of Systems: Considerations for Applications in the Arctic," in *63rd International Astronautical Congress*, Naples, Italy, 2012.

[4] RTCA, *Minimum Operational Performace Standards for the Global Positioning/Wide Area Augment System Airborne Equipment,* RTCA publication DO-229D, 2006.

[5] D. A. Vallado, Fundamentals of Astrodynamics and Applications, 3rd ed., Hawthorne, CA: Microcosm Press, 2007.

[6] GPS Directorate, *Navstar GPS Space Segment/Navigation User Interfaces,* Interface Specification IS-200-GPS, Revision F, 2011.

[7] R. H. Battin, An Introduction to the Mathematics and Methods of Astrodynamics, Revised ed., Reston, VA: AIAA, 1999.

[8] S. Boyd and L. Vandenberge, Convex Optimization, New York, NY: Cambridge University Press, 2004.

[9] Japan Aerospace Exploration Agency, *Quasi-Zenith Satellite System Navigation Service,* Interface Specification for QZSS IS-QZSS V1.4, 2012.